Gamma-Ray Spectroscopy using Germanium Detector

RAHMAT SAEEDI

Physics 397

University of Alberta; Feb 2011

Abstract

Analysis of Compton Scattering (gamma rays of energy 0.03-1.3 MeV) is given for Cs-137, Na-22, and Co-60. The Compton edge was observed in Cs and Na which were in good agreements with theoretical predictions. However due to many multiple scattering in Ba, the Compton edge was not observed for its photopeaks. We present experimental data for attenuation of gamma rays in water at room temperature and ice. The total attenuation coefficient of Cs spectrum in water and ice was found to be 3.3±0.1/meter and 4.6±0.5/meter. Moreover, photopeak attenuation coefficient of Cs was determined to be 9.2±0.5/meter. Finally, inverse-square law was observed in Cs spectrum, indicated by decrease in count rate as the source was moved away from the detector.

1. **Introduction**

Interaction of light and matter has shed lights on our understanding of the nature of atom and much advancement in current technological breakthroughs. For example, applications of photoelectric effect range from everyday digital cameras to photomultipliers used to study nature of subatomic particles at CERN [1]. These interactions could occur at low energies as in thermal interaction and photoelectric effect or at higher energies for instance in Compton scattering and pair productions [2]. In this paper we investigate Compton scattering using a germanium detector, and attenuation of gamma rays in water and ice, finally inverse-square law and its geometrical dependence.

A gamma ray may be scattered without changing its wavelength λ (Bragg scattering) [4] or scattered with a very small Δλ due to thermal agitation [5][6]. Since the energy of phonons is of the order kT, 25meV at ordinary temperatures, [4] much less than gamma energy; hence this energy transfer to electrons is negligible in our experiment. Moreover, pair production require gamma ray of energy greater than 1.02 MeV which shall be negligible in our set up as gamma rays of lower energies was used in most of our experiments.

For reference, if an incident photon of energy E_1 is Compton scattered through and angle θ then by conservation of energy and momentum the followings hold [7][8]:

$$E_e = E_1 - E_2 = E_1 \left(\frac{\frac{E_1}{m_e c^2}(1-\cos\theta)}{1+\frac{E_1}{m_e c^2}(1-\cos\theta)} \right) \quad (1)$$

$$E_2 = \frac{E_1}{1+\frac{E_1}{m_e c^2}(1-\cos\theta)} \quad (2)$$

$$Compton\ Edge = E_c = E_1 \left(\frac{2E_1/m_e c^2}{1+2E_1/m_e c^2} \right) \quad (3)$$

Where c, m_e, E_e and E_2 are respectively speed of light, mass of electron, energy transferred to scattered electron, and energy of the scattered photon.

2. Experimental Details and Results

2.1 Calibration

The detector (see fig. 1) was calibrated using 661.657 KeV photopeak of Cs-137 [9]. Cs-137 was placed inside the detector for 180 seconds (live time, t_{Live}) and the counts at each of the 16383 channels were recorded using the programs Maestro and Ortec Digital Spectrometer. The width of each channel was determined to be 215.9±0.1 eV, where the uncertainty was determined by comparing the double incident photopeak of Cs-137 at 1.323 MeV. Graph 1 show the data collected during this time interval. Note that the data was collected while the temperature of the crystal was lowered to that of liquid nitrogen and high voltage (HV) of 3580±5V was applied to reduce electronic noise and increase sensitivity of the detector.

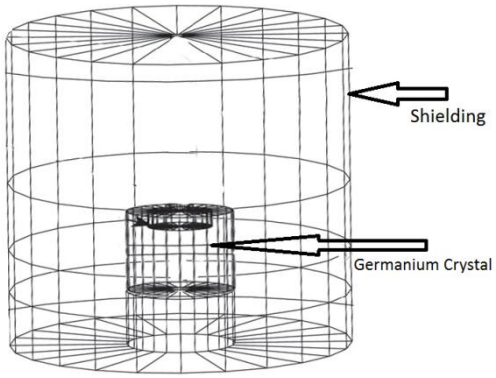

Figure 1: A three dimensional view of the germanium detector and its shielding. The diameter of the crystal was 68±1 mm, with a height of 125±5 mm. The diameter and depth of the cavity was 28±1 cm and 41±1 cm respectively.

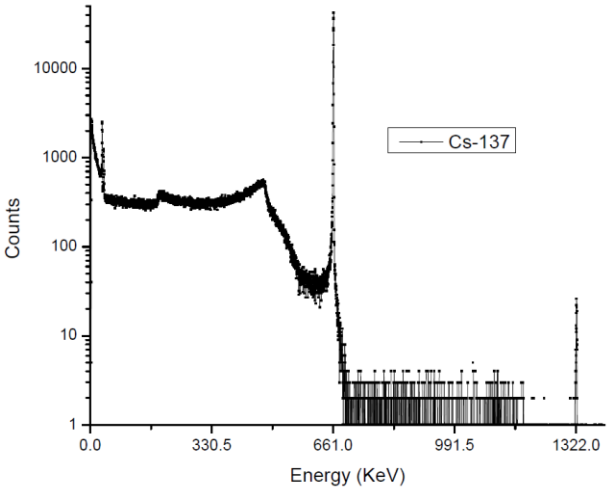

Graph 1: Spectrum of Cs-137, live time of 180 s, is shown which was used to calibrate the detector. The photopeak at 661 KeV and double incident photopeak at 1.32 MeV as well as the Compton edge at 477 KeV is clearly visible.

The Compton edge for Cs-137 was observed to occur at channel 2180 that corresponds to energy of 470.7±0.2 KeV which is 1.4% smaller than the predicted 477.3 KeV value obtained from equation 3. This is believed to be due to electronic losses before integration of voltage by the digital spectrometer.

2.2 Spectra of Some Other Elements

Similar spectrums under HV and reduced temperature and t_{Live}=180s were obtained for Na-22, Co-60, and Ba-133. See graph 2.

Photopeaks of Na-22 was expected to be at 511.0 and 1274.5 KeV [10] and double incident photopeaks at 1022, 1785.5, and 2549 KeV. We observed photopeaks at 510.8±0.3, 1274.8±0.5, 1785.9±0.8 KeV and a hardly recognizable double incident peak at 1022.7±0.5 KeV. The results are in good agreement with the predictions, but no photopeaks was observed at 2549 KeV as the data collected was insufficient to observe this higher energy photopeak. Using equation (3) the Compton edge for the two sodium peaks are expected to be at 340.7 and 1061.7 KeV which are both visible in graph 3.

Photopeaks of Co-60 were expected at 1173.2 and 1332.5 KeV with a double incident peak (the sum-peak) at 2505.7 KeV. The corresponding Compton edges for the single photon incident are 963.4 and 1118 KeV. The observed peaks occurred at 1173.4±0.5, 1332.8±0.6, 2507±1 KeV which agree with predictions. The Compton edges are visible as shown in graph 3 at energies of 957±5 and 1115±5 KeV. Note that no Compton edge was observed for double incident photon, agreeing with theoretical predictions based on negligible probability of absorption two photons by a single electron.

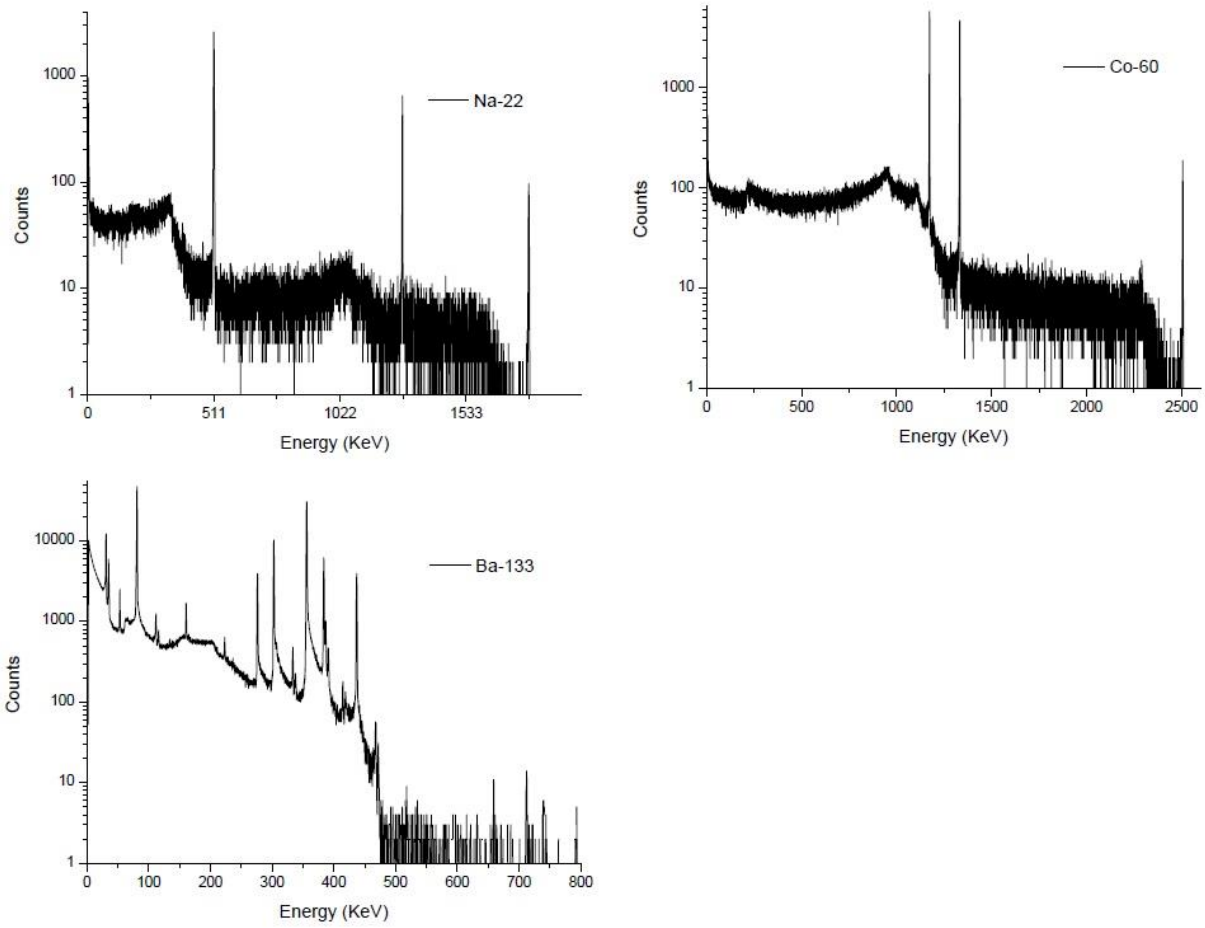

Graph 2: The spectrum of Na-22, Co-60 and Ba-133 is shown above for t_{Live}=180s, HV=3580±5V. The Compton plaque and edge is clearly visible in the case of Na and Co for single incident photopeaks, while in Ba it is harder to observe them.

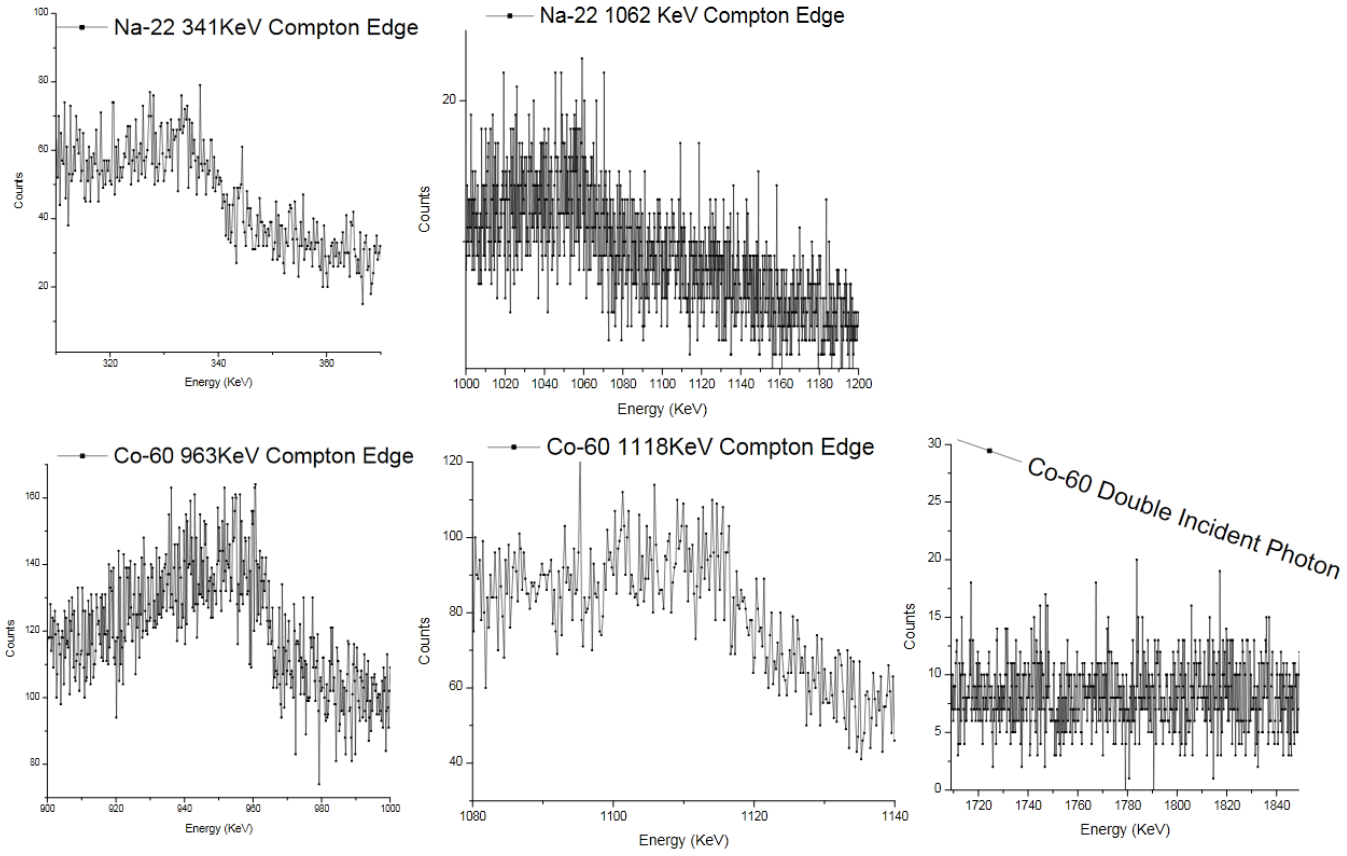

Graph 3: The above graphs show the Compton edge of sodium and cobalt for single photon incident. The values obtained from the graph are in close approximation of predicted values from equation (3). Also note that no Compton edge was observed for the photopeak formed due to double photon incident, in agreement with theoretical prediction.

Finally, a spectrum of Ba-133 was obtained. The single photon photopeaks were expected to occur at 31, 35, 53.16, 79.61, 81.00, 160.61, 223.24, 276.40, 302.85, 356.01, and 383.85 KeV [11] and the multiple photon incidents at energies corresponding to linear integer addition of the above energies. Table 1 compares the experimental and predicted energy for each photopeaks. The theoretical and experimental results are in good agreement.

Table 1: Energies at each photopeak of Ba-133 from graph 2 was determined matched with a probable single or multiple photon incident scattering. The experimental and theoretical values agree.

Channel Number	Energy at that Channel (KeV)	Expected Energy (KeV)	Photons Energy in Multiple Incident (KeV)
145	31.31±0.01	31	
163	35.19±0.02	35	
247	53.33±0.02	53.16	
376	81.18±0.04	81.00	
518	111.84±0.05	112.00	81+31
538	116.15±0.05	116.00	81+35
744	160.63±0.07	160.61	
1034	223.2±0.1	223.24	
1280	276.4±0.1	276.40	
1402	302.7±0.1	302.85	
1545	333.6±0.2	333.85	302.85+31
1564	337.7±0.2	337.85	302.85+35
1649	356.0±0.2	356.01	
1777	383.7±0.2	383.85	
1791	386.7±0.2	387.01	356.01+31
1809	390.6±0.2	391.01	356.01+35
1920	414.5±0.2	414.85	383.85+31
1940	418.8±0.2	418.85	383.85+35
2023	436.8±0.2	437.01	383.85+53.16
2167	467.9±0.2	468.01	356.01+112
2186	472.0±0.2	472.01	356.01+116
3052	658.9±0.3	658.86	356.01+302.85
3299	712.3±0.3	712.02	356.01+356.01
3427	739.9±0.3	739.86	383.85+356.01
3674	793.2±0.4	793.02	53.16+356.01+383.85

2.3 Gamma Ray Attenuation

It is known that placing an object in the pathway of gamma rays would result in attenuation of the ray. In the gamma ray region; attenuation is governed by the usual relation $I = I_0 e^{-\mu x}$ where μ and x are attenuation coefficient and length of the material in the path of the gamma rays, respectively. Height of water in a beaker was varied and it was placed between Cs-137 and the detector, while keeping the distance of Cs from detector fixed and applying HV to liquid nitrogen cooled crystal. Spectrum was collected for t_{Live}=180.0s.

Two different techniques were used to amylase the data. In the first method the total counts of the rays was determined by summing over the counts of all channels. The data was then linearized and graphed, finally finding the attenuation coefficient to be 3.3±0.1/meter from its slope. In the second method, the total counts underneath the photopeak was determined by defining photopeak to be 21 channels wide region whose center coincide with channel having the highest counts in that region. Then a Gaussian graph was fitted to the region and the area underneath was found using OriginLab software. Finally, the data was linearized and attenuation coefficient was found to be 9.2±0.5/meter. Note that the photopeak attenuation is about 3 times that of total attenuation coefficient. This indicates that many of the gamma rays scatter in water, and then these scattered photons are detected by germanium crystal which now have a smaller energy. Moreover, the linearized graphs are in agreement with exponential attenuation of the rays -see graph 4 and 5. Finally, the arbitrary 21 channel wide photopeak has little influence on the conclusions made about the trends of the data. Using the first technique, total attenuation of gamma rays in blocks of ice were found to be 4.6±0.5/meter, slightly higher than total attenuation in water (See graph 6).

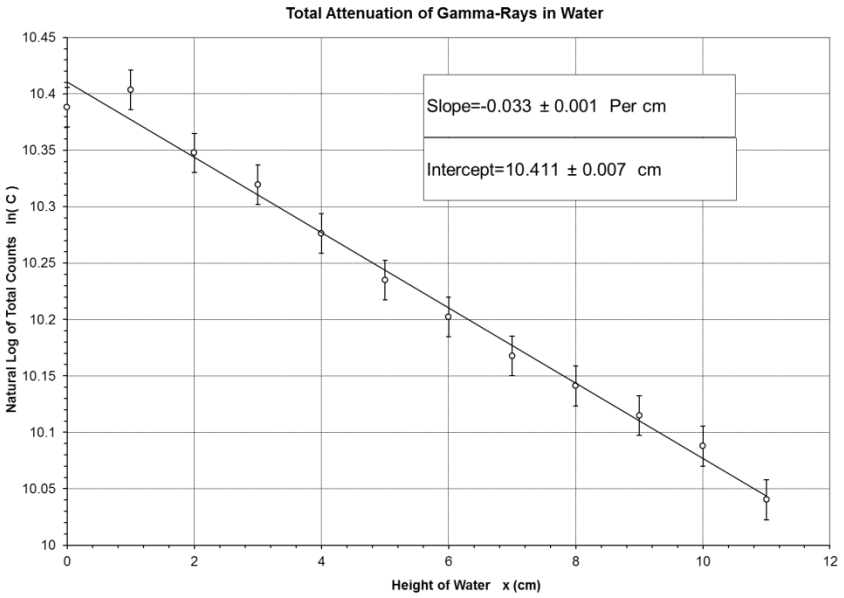

Graph 4: Total attenuation of gamma rays in water is shown in the graph. Total count was determined by summing the counts of each channel for the whole spectrum. The total attenuation coefficient is found to be 3.3±0.1/meter. Y-intercept represents the total counts of the spectrum when there is no water in-between the detector and the source.

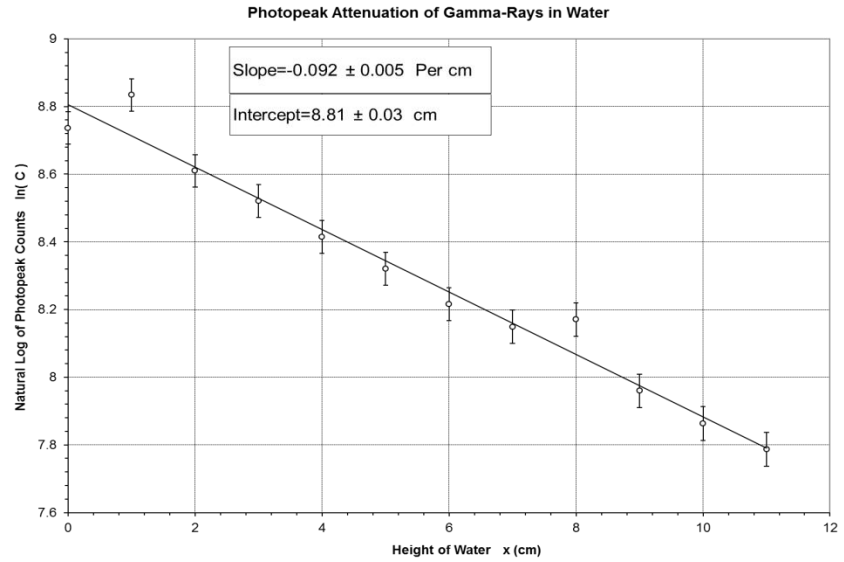

Graph 5: Photopeak attenuation of gamma rays in water is shown in the graph. The photopeak was assumed to be 21 channels wide and photopeak count was determined by integrating under Gaussian fit of the photopeak. The photopeak attenuation coefficient is found to be 9.2±0.5/meter which is 3 times that of total attenuation coefficient.

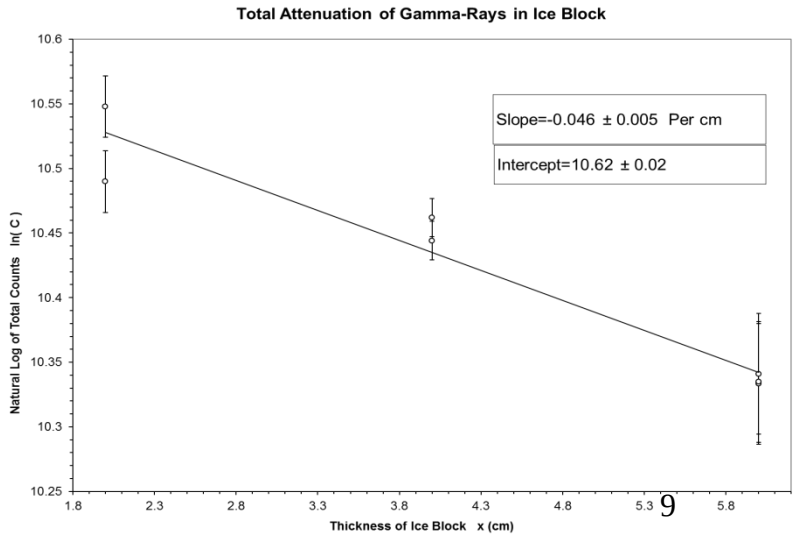

Graph 6: Total attenuation of gamma rays in Ice is shown in this graph. The total attenuation coefficient is found to be 4.6±0.5/meter which is higher than total attenuation coefficient of water.

2.4 Geometrical Effects and $^{1}/_{r^2}$ Law

A sample of Cs-137 was placed inside the detector at a fixed horizontal distance from the crystal. The height of the sample (from bottom of the detector) was varied and spectrum of Cs was collected. HV, live time, and temperature of the crystal were kept the same. Four spectrums for heights corresponding to 40.0±0.5, 26.0±.5, 6.8±0.5, and 7.0±0.5 cm were collected (see Graph 7 and Table 2). The result reveals decrease in count rate as the height (therefore the distance from the center of crystal) increased. This inverse relation is due to $^{1}/_{r^2}$ law. Also, deformed Compton plaque and Compton edge was observed which is believed to be due to combined effect of inverse-square law and path length of the ray inside the crystal. Further improvements in this section of the experiment are required as quantitative measurements could not be found. To improve this experiment, more accurate measurement of crystal dimensions, positioning of the sample is essential.

Sample Height (cm)	Total Counts	Maximum Counts at Photopeak
40.0±0.5	13851	391
26.0±0.5	28633	691
6.8±0.5	52784	1393
7.0±0.5	52829	1365

Table 2: As the height of the sample was increased, the average and photopeak count rate photopeak decreased. This could be due to

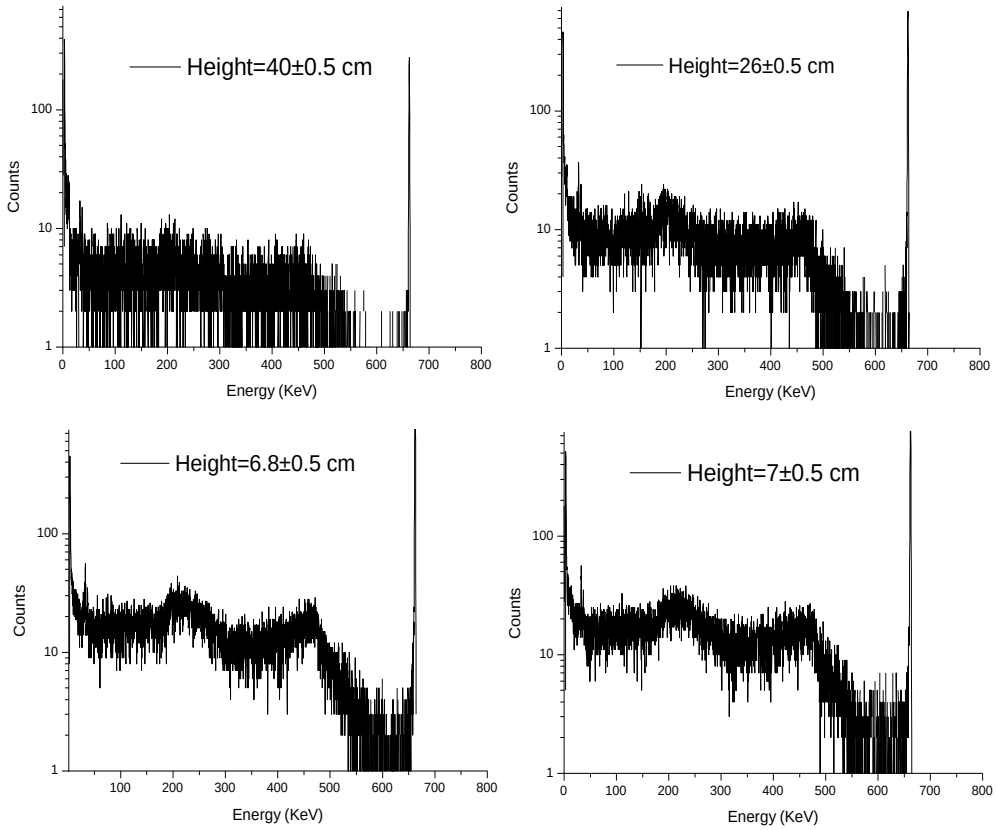

Graph 7: Height of a sample of Cs-137 in a detector from the bottom of the detector was varied and spectrum of it was collected for 180.0s. The graphs show that the count rate of at each channel decreases which is believed to be mainly due to inverse square law for the gamma rays. Also, the Compton plaque deforms which is believed to be due to decrease path length of gamma rays in the crystal and inverse $1/r^2$ law.

Conclusion

We conclude that even though gamma ray spectrums are probabilistically governed, the Compton scattering satisfactory explains the trends of gamma ray spectrum in the long run given the energies of incoming photons is known. We also report values 4.6±0.5/m and 3.3±0.1/m for total spectra attenuation coefficient of ice and water at room temperature for gamma rays.

Moreover, attenuation coefficient for photopeak of Cs-137, (661KeV) was determined to be 9.2±0.5/m. Finally, we report on observation of inverse-square law and geometrical dependence of gamma-ray spectra. The next step in our experiments is to study wave-particle duality and interaction using single photon interference.

Acknowledgments

We thank Dr. Hallin for helpful discussions on germanium detector and Vlad, Taylor and Lorne for technical assistance and making available necessary equipment to perform this experiment.

References

[1] S. Chatrchyan *et al*; Study of Various Photomultiplier Tubes with Muon Beams And C˘ erenkov Light Produced in Electron Showers; CMS Note; Cern March 2010
[2] C. H. Lee, W. T. Hill; Light-Mater Interaction; ISBN 978-3-527-40661-6 (2007)
[4] H. Curien; Compton Scattering of X-Rays in Crystals; Reviews of Modern Physics, V30, Number 1 (1958)
[5] J. Laval, Rayons X et structures atomiques (Collège de France, Paris, 1948)
[6] J. Laval, Bull. soc. Franç. Minèral, 64, 1 (1943)
[7] P. A. Tipler, R. A. Llewellyn; Modern Physics, 5th Edition; ISBN 0-7167-7550-6; Pg. 137 (2008)
[8] K. Howley; Gamma-Ray Spectroscopy; Lawrence Livermore National Lab (2003)
[9] E. BROWNE, J. K. TULI; Nuclear Data Sheets 108,2173 (2007); www.nndc.bnl.gov
[10] R.B. FIRESTONE; Nuclear Data Sheets 106, 1 (2005); www.nndc.bnl.gov
[11] SHAHEEN RAB; Nuclear Data Sheets 75,491 (1995); www.nndc.bnl.gov